FULL PAPER

BJC

British Journal of Cancer (2013) 109, 433–443 | doi: 10.1038/bjc.2013.325

Keywords: apoptosis; endoplasmic reticulum stress; GRP78; melanoma; glioblastoma; neuroblastoma

Inducing apoptosis of cancer cells using small-molecule plant compounds that bind to GRP78

S Martin[1], H K Lamb[2], C Brady[1], B Lefkove[3,4], M Y Bonner[3,4], P Thompson[2], P E Lovat[5], J L Arbiser[3,4], A R Hawkins[2] and C P F Redfern*[,1]

[1]Newcastle Cancer Centre at the Northern Institute for Cancer Research, Medical School, Newcastle University, Newcastle upon Tyne NE2 4HH, UK; [2]Newcastle University Protein Purification and Characterisation Unit, Institute of Cell and Molecular Biosciences, Medical School, Newcastle University, Newcastle upon Tyne NE2 4HH, UK; [3]Department of Dermatology, Emory University School of Medicine, Atlanta, GA 30322, USA; [4]Atlanta Veterans Administration Medical Center, WMB 5309, 1639 Pierce Drive, Atlanta, GA 30322, USA and [5]Institute of Cellular Medicine, Medical School, Newcastle University, Newcastle upon Tyne NE2 4HH, UK

Background: Glucose regulated protein 78 (GRP78) functions as a sensor of endoplasmic reticulum (ER) stress. The aim of this study was to test the hypothesis that molecules that bind to GRP78 induce the unfolded protein response (UPR) and enhance cell death in combination with ER stress inducers.

Methods: Differential scanning calorimetry (DSC), measurement of cell death by flow cytometry and the induction of ER stress markers using western blotting.

Results: Epigallocatechin gallate (EGCG), a flavonoid component of Green Tea *Camellia sinensis*, and honokiol (HNK), a *Magnolia grandiflora* derivative, bind to unfolded conformations of the GRP78 ATPase domain. Epigallocatechin gallate and HNK induced death in six neuroectodermal tumour cell lines tested. Levels of death to HNK were twice that for EGCG; half-maximal effective doses were similar but EGCG sensitivity varied more widely between cell types. Honokiol induced ER stress and UPR as predicted from its ability to interact with GRP78, but EGCG was less effective. With respect to cell death, HNK had synergistic effects on melanoma and glioblastoma cells with the ER stress inducers fenretinide or bortezomib, but only additive (fenretinide) or inhibitory (bortezomib) effects on neuroblastoma cells.

Conclusion: Honokiol induces apoptosis due to ER stress from an interaction with GRP78. The data are consistent with DSC results that suggest that HNK binds to GRP78 more effectively than EGCG. Therefore, HNK may warrant development as an antitumour drug.

A fundamental property of all cells is their ability to adapt and survive despite variation in environmental conditions. Minimising errors in the conformational integrity of proteins, vital to the functioning of the endoplasmic reticulum (ER), is achieved via the unfolded protein response (UPR); this homeostatic mechanism is induced by ER stress resulting from any disruption to protein production, folding or degradation. The ER-resident protein, glucose regulated protein 78 (GRP78), functions as a sensory hub and is present as complexes with three proteins: the protein kinase-like ER kinase (PERK or eukaryotic initiation factor 2 alpha kinase 3), inositol-requiring element 1 (IRE1) and activating transcription factor 6 (ATF6) (Schroder, 2005, 2006). Glucose regulated protein 78 also possesses high affinity for hydrophobic or hydrophilic regions exposed on the surface of unfolded or

*Correspondence: Dr CPF Redfern; E-mail: chris.redfern@newcastle.ac.uk

Received 23 April 2013; revised 30 May 2013; accepted 4 June 2013; published online 27 June 2013

misfolded protein substrates; these interactions can be modulated by the binding of ADP and ATP to an N-terminal ATP-binding domain, and result in dissociation and activation of PERK, IRE1 and ATF6 (Bertolotti *et al*, 2000; Shen *et al*, 2002). Dissociation of ATF6 facilitates Golgi-mediated processing of ATF6 to an active transcription factor; the dissociation of PERK and the endoribonuclease precursor IRE1 from GRP78 allows oligomerisation and auto-phosphorylation to form active kinases (Schroder and Kaufman, 2005; Schroder, 2005, 2006). Protein kinase-like ER kinase, IRE1 and ATF6 are key UPR regulators that initiate downstream responses of ER stress including the cessation of cap-dependent mRNA translation, the induction of chaperones to assist in protein folding and the induction of apoptosis via activating transcription factor 4 (ATF4) and GADD153/CHOP (Blais *et al*, 2004).

The expression of GRP78 may be enhanced in metastatic cells and late-stage tumours, and its role as an ER stress sensor suggests that it may be useful as a therapeutic target (Lee, 2007; Martin *et al*, 2010). Although siRNA-mediated knockdown of GRP78 increases cell death *in vitro* (Virrey *et al*, 2008), this may be difficult to achieve *in vivo* and alternative approaches to inhibiting GRP78 may be more effective as therapeutic strategies. The N-terminal ATPase domain important to GRP78 function also forms complexes with procaspases thus preventing caspase activation; this interaction can be abrogated with dATP to increase drug-induced cell death (Rao *et al*, 2002; Reddy *et al*, 2003). Treatment with nucleoside analogues that bind to the ATPase domain and facilitate dissociation of GRP78/procaspase complexes and disrupt the ability of GRP78 to bind/release substrates may, therefore, be a useful strategy to inhibit GRP78. Additional approaches may be to use natural inhibitors, such as the Green Tea *C. sinensis* flavonoid epigallocatechin gallate (EGCG) (Ermakova *et al*, 2006) or cytotoxin-mediated cleavage by AB_5 Subtilase ($SubAB_5$) (Paton *et al*, 2006; Paton and Paton, 2010). Epigallocatechin gallate blocks the ATPase domain of GRP78 (Ermakova *et al*, 2006) and enhances cell death in response to temozolamide or etoposide (Virrey *et al*, 2008). Epigallocatechin gallate also inhibits the 26S proteasome and NFκB signalling cascade and, while clearly not specific to GRP78, may be a candidate drug to overcome chemoresistance in solid tumours (Nam *et al*, 2001; Ermakova *et al*, 2006).

There may be other natural products that could be used to inhibit GRP78. Honokiol (2-(4-hydroxy-3-prop-2-enyl-phenyl)-4-prop-2-enyl-phenol) (HNK), a cell-wall component of *M. grandiflora,* is a potent antitumorigenic and neurotrophic compound (Chen *et al*, 2010), which induces apoptosis as a result of ER stress in chondrosarcoma cells with the concomitant upregulation of GRP78. Unpublished proteomic data have suggested that HNK binds to GRP78 and the aim of this study was to investigate the binding of HNK and EGCG to GRP78, and characterise the effect of these as single agents on neuroectodermal tumour cells and in combination with two drugs, fenretinide and bortezomib, known to induce ER stress-induced cell death.

MATERIALS AND METHODS

Growth and maintenance of cell lines. CHL-1 and WM266-4 (ATCC #; CRL-9446, CRL-1676) human melanoma and U251 and MO59J human glioblastoma cell lines were cultured in high glucose ($4.5\,g\,l^{-1}$) DMEM supplemented with 10% FBS (Sigma-Aldrich, Poole, UK). SH-SY5Y and NGP human neuroblastoma cell lines were cultured in RPMI-1640 medium (Sigma-Aldrich) supplemented with 10% FBS. Murine SVR angiosarcoma cells (Arbiser *et al*, 1997) were cultured in DMEM/10% FBS. Cells were maintained at 37 °C in a humidified atmosphere of 5% CO_2 in air to a maximum of 50 passages.

Plasmid construction and purification of recombinant GRP78. The coding sequence of murine GRP78 lacking the signal peptide was synthesised by Blue Heron Biotech LLC (Bothell, WA, USA) and subcloned into 5′*Nde*1 and 3′*Bam*H1 sites of the *E. coli* expression vector pET15b to produce plasmid pMUT177. The amino-acid sequences of the nucleotide-binding domains (NBDs) of murine and human GRP78 differ by a single substitution. The complete amino-acid sequence of the GRP78 encoded by pMUT177 is shown in Supplementary Figure 1. Glucose regulated protein 78 was overproduced in *E. coli* and purified as described previously (Lamb *et al*, 2006) but with additional chromatographic purification through hydroxyapatite: protein in 50 mM K phosphate pH 7.2, 1 mM DTT was loaded onto a hydroxyapatite column, washed with buffer to remove unbound protein and GRP78 eluted with a linear gradient of 50–400 mM K phosphate pH 7.2, 1 mM DTT.

Differential scanning calorimetry (DSC) and isothermal titration calorimetry (ITC). The methodology and rationale for DSC and ITC analysis are summarised in Lamb *et al* (2006) and references contained within. Although some GRP78 molecules may have nucleotide bound at the end of the purification, this will be released from the protein before the protein unfolding (Cooper, 2001).

Affinity separation and identification of proteins binding to biotinylated HNK. Biotinylation of HNK was achieved by incubating 0.187 mmol of HNK in a dry round-bottomed flask, containing 5 ml of chloroform and 1 ml of dimethylformamide, with 0.375 mmol of pentafluorophenyl–biotin at 40 °C with stirring for 30 min, and then 1 h at room temperature. Chloroform and pentafluorophenol were removed at 33 °C by rotary evaporation, and the solid dried under high vacuum overnight. SVR angiosarcoma cells were washed in 10 ml Dulbecco's phosphate-buffered solution, trypsinised in 1 ml trypsin–EDTA (0.05% trypsin and 0.53 mM EDTA), resuspended in 10 ml DMEM and pelleted by centrifugation. Whole-protein isolates were obtained by resuspending the cells in 20 mM Tris HCl (pH 7.5), 150 mM NaCl, 1% (v/v) Triton X-100, 10% glycerol, 1 mM EDTA, $10\,\mu g\,ml^{-1}$ leupeptin, $10\,\mu g\,ml^{-1}$ aprotinin, 1 mM benzamidine, 1 mM PMSF and 1 mM Na_3VO_4, followed by centrifugation at 15 000 r.p.m. in an Eppendorf (Hauppauge, NY, USA) 5415C microcentrifuge. Approximately 1 mg of protein was incubated with biotinylated HNK for 3 h at 37 °C and the mixture incubated with 150 μl of M-270 Streptavidin beads (Dynal Biotech, Invitrogen, Grand Island, NY, USA) for 2 h at 37 °C. Beads were collected using a magnetic field, washed three times with PBS and proteins eluted by denaturation at 100 °C for 10 min followed by centrifugation at 13 000 r.p.m. Thirty microlitre of the eluate was analysed on a 10% Tris-SDS polyacrylamide gel, and bands were excised and digested overnight with Trypsin at 37 °C. Peptides were extracted, desalted (50% of sample) using C18 ZipTip (Millipore, Billerica, MA, USA) and analysed using an Ultimate nano HPLC LC-MS/MS (Dionex/LC Packings, CA, USA) with a FAMOS autosampler and SWITCHOS column switcher for online desalting, interfaced to a QSTAR XL mass spectrometer (Applied Biosystems, Foster City, CA, USA). Elution from the column was accomplished with an acetonitrile gradient from 2–80% with 0.1% formic acid as a counter ion for HPLC. The flow rate was $275\,nl\,min^{-1}$. MS/MS data were processed by MASCOT using the SwissPROT database using mammals as a limit on the species. Ion scores were calculated as $-10*\mathrm{Log}(P)$, where P is the probability that the observed match is a random event. Individual ion scores >33 indicate an identity or an extensive homology. Only proteins with ProtScore >1.0 ($>85\%$ confidence) were considered.

Drug preparation and treatment regimes. EGCG and HNK were added to cell cultures, alone or in combination with the ER stress inducers fenretinide or bortezomib, dissolved in an appropriate

vehicle (⩽0.01% of culture volume); an equal volume of vehicle was used to treat control cells. Epigallocatechin gallate (Sigma-Aldrich) was dissolved in PBS; HNK (Sigma-Aldrich) and bortezomib (Velcade; Millenium, Janssen-Cilag Ltd, High Wycombe, UK) were dissolved in DMSO; and fenretinide (Janssen-Cilag Ltd, Zug, Switzerland) was dissolved in ethanol. In combination experiments, for melanoma and glioblastoma cell lines, fenretinide and bortezomib were used over concentration ranges of 1–20 μM and 0.01–0.4 μM, respectively, with ratios of 1 : 1 for fenretinide with EGCG, 1 : 5 for fenretinide with HNK, 1 : 50 for bortezomib with EGCG and 1 : 250 for bortezomib with HNK. Neuroblastoma cell lines were more sensitive to these drugs, and fenretinide and bortezomib were used at concentration ranges of 1–10 μM and 0.01–0.04 μM, respectively, with ratios of 1 : 2 for fenretinide with EGCG, 1 : 10 for fenretinide with HNK, 1 : 500 for bortezomib with EGCG and 1 : 2500 for bortezomib with HNK.

Measurement of cell death by flow cytometry and cell viability assays. Cells were seeded into 6-well plates (Corning; Sigma-Aldrich) at densities of 1.5×10^5 (CHL-1), 2.0×10^5 (U251, MO59J, SH-SY5Y and NGP) or 2.5×10^5 (WM266-4) cells per well and attached overnight at 37 °C. After treatment, cells and supernatant were harvested and analysed by flow cytometry as described previously (Martin *et al*, 2010) using either FACScan or FACScalibur flow cytometers (Becton Dickinson Immunocytometry Systems, Oxford, UK) to determine the percentage of cells with hypodiploid DNA (subG1 peak) as a measure of cell death. CellTiter 96 Aqueous One Solution Reagent (Promega, Southampton, UK; MTS assay) was used to measure viability of 5000 cells per well in flat-bottomed 96-well tissue culture plates after treatment for 24 h according to the manufacturer's instructions. Epigallocatechin gallate is auto-fluorescent at the wavelength used for CellTiter 96 Aqueous One Solution reagent (490 nm), and the Sulphorodamine B colorimetric cytotoxicity assay (SRB assay; (Haselsberger *et al*, 1996)) was used instead.

Western blot analysis for protein expression. Proteins were extracted from cell pellets, quantified using Bradford assay reagent (Pierce Biotech., Rockford, IL, USA), separated by electrophoresis through 4–20% Tris-glycine polyacrylamide gels (Bio-Rad Laboratories, Hemel Hempstead, UK) and blotted as described previously (Armstrong *et al*, 2010). Blots were probed with antibodies, diluted in 5% non-fat milk (in TBS/Tween) to appropriate concentrations, for either 1 h at room temperature or 4 °C overnight (Armstrong *et al*, 2010). Antibodies were for the GRP78 C-Terminus (Santa Cruz Biotechnology, Heidelberg, Germany; 1 : 1000 dilution), ATF4 (Santa Cruz Biotechnology; 1 : 500 dilution), Cleaved Caspase 3 (Cell Signalling Technology, Danvers, MA, USA; 1 : 500 dilution) and β-actin (Sigma-Aldrich; 1 : 5000 dilution). Detection and visualisation was by horseradish peroxidase-conjugated secondary antibodies (Upstate Biotechnology, Boston, MA, USA; diluted 1 : 2000) and the ECL-plus system (Amersham Biosciences, Little Chalfont, UK) with imaging on a Fujifilm FLA-3000 fluorescence imager (Raytek Scientific Ltd, Sheffield, UK). Densitometric quantification of signal intensity relative to the β-actin loading control was performed using Aida Image Analyser version 3.28 software (Raytek Scientific Ltd.).

Statistical analysis. Results were expressed as the mean of individual experiments ± 95% confidence intervals (95% CI) using Prism 5 (GraphPad Software Inc., La Jolla, CA, USA) or Sigma Plot 11 (Systat Software Inc., San Jose, CA, USA) software. Responses were compared by one- or two-way ANOVA with either Dunnett's or Bonferroni's *post-hoc* tests using Prism 5 or SPSS release 17.0 (IBM, Chicago, IL, USA) software. To analyse the synergistic effects of fenretinide and bortezomib alone or in combination with GRP78 inhibitors on induction of cell apoptosis or inhibition of cell viability, combination indices (ci) were generated using CalcuSyn software (Biosoft, Cambridge, UK) as previously described (Corazzari *et al*, 2003) and used to assess whether drug combinations were additive (ci ≈ 1), inhibitory (ci > 1) or synergistic (ci < 1) with respect to cell death. Combination index data were ranked and analysed using R (R Development Core Team, 2012), initially with linear models to test for the effect of drug dose (not significant; $P > 0.05$) and then by nested ANOVA (cell line nested within cell type); pairwise comparisons of mean ci by cell line or cell type (depending on the results from the nested ANOVA) were carried out using Tukeys HSD after one-way ANOVA. Q–Q plots were used to assess the fit of residuals from the models. Interpretation of dose–response curves for estimation of EC_{50} and asymptote were carried out using R and the package drc (Ritz and Streibig, 2005).

RESULTS

Affinity separation of proteins from cell-free lysates using biotinylated HNK. EGCG–Sepharose 4B affinity chromatography experiments with a nested set of overlapping N-terminally deleted GRP78 proteins have implied that EGCG binds to the NBD within GRP78 (Ermakova *et al*, 2006). In the current work, affinity separation experiments with biotinylated HNK resulted in the identification of GRP78 as a component of murine SVR angiosarcoma cells, which bound HNK; MASCOT alignment showed local sequence matches to GRP78 with ion scores 47, 55 and 73, respectively. The protein score, derived from the ion scores as a non-probabilistic basis for ranking protein hits, was 175. Peptides corresponding to the HSP-70 isoform 1, a protein with extensive homology to GRP78, three keratins and a calreticulin-binding and neural-survival protein DSEP were also identified (Table 1).

EGCG and HNK bind to the unfolded form of the NBD of GRP78. Using DSC, we have shown previously that GRP78 unfolds in two thermal transitions, the first corresponding to the NBD and the second to the substrate-binding domain (SBD) (Lamb *et al*, 2006). To characterise the binding of EGCG and HNK to GRP78, DSC was used to unfold GRP78 in the absence and presence of EGCG (0.2 and 1.0 mM) or HNK (0.1 mM and 0.2 mM; Figure 1). In each case, EGCG and HNK bound with the greatest affinity to the NBD as judged by the relative changes in the melting temperature (Tm) of the NBD and SBD domains (Figure 1; Table 2). The changes in Tm were negative, implying that EGCG and HNK were bound to the unfolded form of GRP78.

Table 1. Identification of peptides binding to biotinylated honokiol in SVR angiosarcoma cell extracts

Protein	Protein score	Peptide hits (ion score >33)
Keratin 1	633	10
HSC71	529	9
Serum albumin	206	5
CK2e	193	4
GRP78	175	3
Igα1-C	112	3
Keratin 9	90	2
DSEP	63	1

For simplicity, only hits corresponding to proteins in the human database are given; four additional peptides corresponding to unidentified human proteins were also present. We note that keratin 1 is a component of the kininogen receptor complex on endothelial cells and is frequently found in angiosarcomas (Remotti *et al*, 2001).

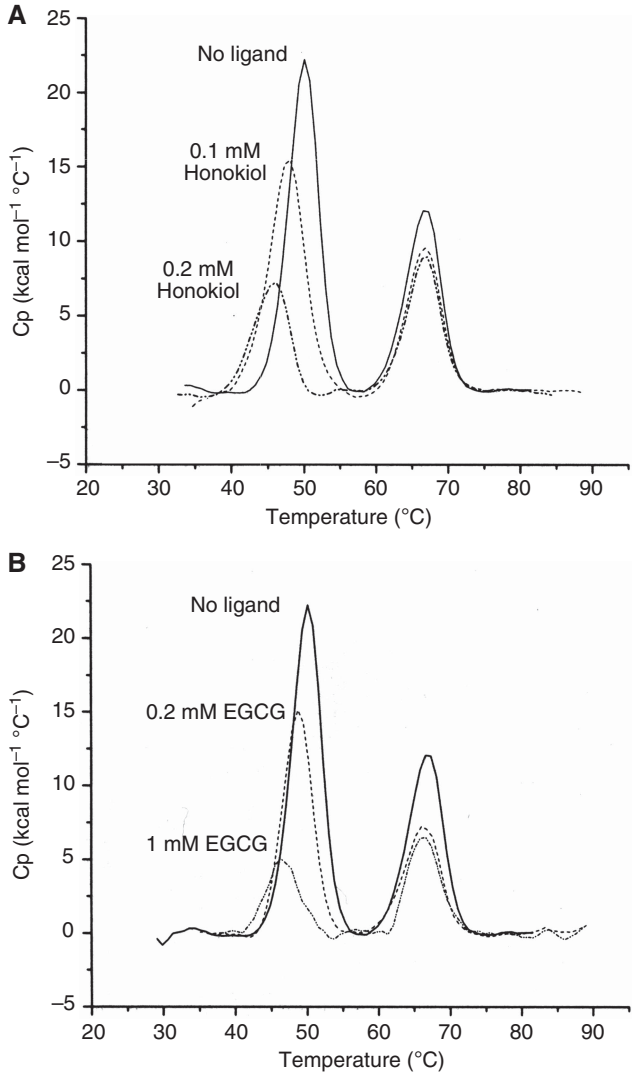

Figure 1. GRP78 (10 μM) in 50 mM HEPES, 0.1 M KCl and 1 mM β-mercaptoethanol pH 7.2 was subject to thermal denaturation in the presence or absence of honokiol (**A**) or EGCG (**B**). Samples were heated from 25–80 °C at a rate of 90 °C per hour. Solid lines, no ligand; dashed lines, 0.1 mM honokiol (**A**) or 0.2 mM EGCG (**B**); dashed and dotted lines, 0.2 mM honokiol (**A**) or 1 mM EGCG (**B**).

This interpretation was tested directly by ITC experiments at 25 °C where the titration of 1 mM HNK or EGCG into 35 μM GRP78 gave no significant heat exchanges above background heat of dilution (data not shown) implying no binding to folded GRP78. As thermal transitions in the DSC experiments are not reversible, binding data cannot be deconvoluted to derive binding constants. However, DSC data for EGCG and HNK were consistent with the interpretation that HNK has a relatively greater affinity for GRP78 than does EGCG.

EGCG has been reported to bind to several proteins (cited in Ermakova *et al* (2006)); therefore, we used DSC with *Escherichia coli* DnaK (a member of the HSP-70 chaperone family that includes GRP78), human thymidylate kinase and *Aspergillus nidulans* NmrA (an NAD-binding transcription repressor involved in nitrogen metabolism) (Stammers *et al*, 2001; Lamb *et al*, 2003; Zhao *et al*, 2010) to test the possibility that HNK is promiscuous with respect to protein-binding activity. In all cases tested, HNK preferentially bound to the unfolded form of the protein as demonstrated by the reduction in the Tm of the thermal transitions in the presence of HNK (Figure 2 in the Supplementary Material).

Table 2. The binding of honokiol and EGCG to GRP78

	Tm1 NBD (°C)	ΔTm (°C)	Tm2 SBD (°C)	ΔTm (°C)
No ligand	50.0 ± 0.1		66.6 ± 0.4	
0.1 mM honokiol	47.5 ± 0.3	− 2.5	66.1 ± 0.1	− 0.5
0.2 mM honokiol	45.4 ± 0.1	− 4.6	66.6 ± 0.4	0
0.2 mM EGCG	48.6 ± 0.1	− 1.4	66.1 ± 0.1	− 0.5
1 mM EGCG	46.7 ± 0.3	− 3.3	66.2 ± 0.2	− 0.4

Abbreviations: DSC = differential scanning calorimetry; EGCG = epigallocatechin gallate; NBD = nucleotide-binding domain; SBD = substrate-binding domain; Tm = melting temperature. GRP78 (10 μM) in 50 mM HEPES, 0.1 M KCl and 1 mM β-mercaptoethanol pH 7.2 was subject to thermal denaturation in a VP-DSC microcalorimeter in the presence or absence of honokiol or EGCG at the concentrations stated. Samples were heated from 25–80 °C at a rate of 90 °C per hour. The results shown are the average of triplicate DSC scans and include the s.d. Tm1 corresponds to the midpoint of the transition for the NBD and Tm2 for the SBD.

Thus, HNK is promiscuous in its ability to bind to unfolded proteins but the differential lowering of the Tm for the GRP78 NBD and SBD (see Table 2) seen when GRP78 is unfolded in the presence of HNK implies a range of affinities for different amino-acid sequences.

ER stress and death of neuroectodermal tumour cells in response to EGCG or HNK. Fenretinide and bortezomib induce ER stress leading to cell death, mediated by ATF4 induction, in neuroectodermal tumour cells (Armstrong *et al*, 2010). Using a panel of neuroectodermal tumour cells (CHL-1 and WM266-4 melanoma; U251 and MO59J glioblastoma; and NGP and SH-SY5Y neuroblastoma), we investigated the properties of EGCG and HNK with respect to the induction of cell death and inhibition of viability in comparison with fenretinide and bortezomib. All four compounds induced cell death to varying degrees (Figure 2). While EGCG was relatively consistent in producing sigmoidal dose–response curves for cell death, the dose–response kinetics for HNK varied between cell types (Figure 2). In addition, HNK produced marked hormetic responses (stimulation of cell growth at low doses) on cell viability in all cell lines, which were not apparent with EGCG. The half-maximal effective concentrations (EC50) and maximal level of cell death (asymptote) for each compound are summarised in Table 3. With respect to EC50, sensitivity to each drug was cell-line specific, with neuroblastoma cells (NGP and SH-SY5Y) the most sensitive compared with the melanoma or glioblastoma cells. Across cell lines, EC50 values for HNK ranged from 15–56 μM; for EGCG EC50 values ranged from 4.6–51 μM but there was less consistency within cell types (melanoma, glioblastoma and neuroblastoma) compared with HNK. Asymptotes of the dose–response curves for each cell line (maximal levels of cell death) differed between drugs (one-way ANOVA on ranks, $P<0.01$) with EGCG producing lower mean levels of cell death at maximum dose (26%) than fenretinide (62%) or HNK (51%; Tukey's HSD, $P=0.011$, Table 3). There was no correlation between EGCG and HNK with respect to their EC50 or asymptote values across cell lines (Pearson correlation coefficients <0.25; $P>0.6$).

Using the induction of GRP78 and ATF4 proteins as markers of ER stress and UPR activation (Samali *et al*, 2010), and caspase-3 cleavage as a marker of apoptosis (Figure 3), in dose–response experiments HNK induced caspase-3 cleavage and the expression of ATF4 and GRP78 in all six cell lines; the kinetics of induction with respect to HNK dose and the induction of cell death were

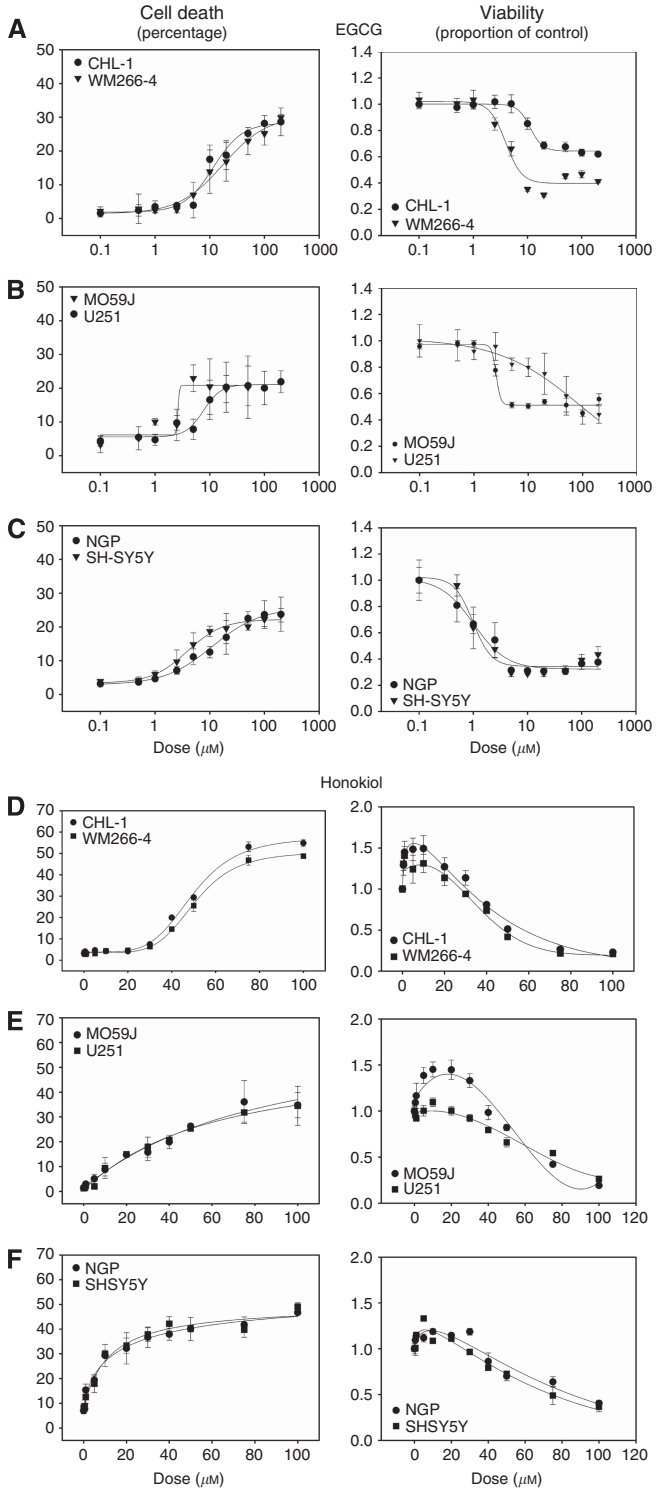

Figure 2. The effect of EGCG or honokiol on neuroectodermal tumour cell lines. Melanoma (**A** and **D**), glioblastoma (**B** and **E**) and neuroblastoma (**C** and **F**) cells were treated with increasing doses (EGCG: dose range = 0.1–200 μM; HNK, dose range = 0.1–100 μM) for 24 h and assessed for induction of cell death (% subG1 fraction from flow cytometry; each point is the mean percentage SubG1 peak of three experiments ± 95% CIs) and inhibition of cell viability (relative viability; MTS assay or SRB assay, eight replicate experiments ± 95% CI). For all cell death graphs (left column, the ordinate scales are percentage cell death) and for viability graphs (right column), the ordinate scales are viability as a proportion of control.

Table 3. Estimated EC50 (μM) and asymptotes (percentage cell death) for the induction of cell death in neuroectodermal tumour cell lines

	EC50				Asymptote			
Cell line	**FenR**	**Bort**	**EGCG**	**HNK**	**FenR**	**Bort**	**EGCG**	**HNK**
CHL-1	38.48	0.12	10.30	49.10	90.35	30.37	24.20	61.30
WM266-4	9.08	0.21	51.20	51.00	36.30	31.61	36.40	51.80
MO59J	13.07	0.22	4.60	56.20	81.03	46.94	21.10	53.10
U251	12.23	2.44	9.00	37.30	78.48	100.00	21.00	40.30
NGP	3.05	0.02	5.70	15.30	32.53	34.53	29.80	49.50
SH-SY5Y	5.24	0.01	18.60	14.60	52.82	44.09	23.40	51.10
Median	10.65	0.17	9.65	43.20	65.65	39.31	23.80	51.45
Mean	13.53	0.50	16.57	37.25	61.92	47.92	25.98	51.18

Abbreviations: Bort = bortezomib; EGCG = epigallocatechin gallate; FenR = fenretinide; HNK = honokiol. Comparison of ranks for EC50: by nested ANOVA (cell line within cell type, melanoma, glioblastoma or neuroblastoma), no significant effect of cell line (cell type:cell line interaction, $P = 0.95$) but significant differences between cell lines with neuroblastoma cell lines being significantly more sensitive to all drugs than melanoma or glioblastoma (Tukey's HSD, $P < 0.02$) and no significant difference between melanoma and glioblastoma ($P = 0.93$).

similar across cell lines, although ATF4 was induced relatively earlier in WM266-4 melanoma cells (Figure 3). The magnitude of relative induction of the ER stress marker ATF4 in response to HNK was substantially and consistently lower than with bortezomib but comparable or in excess of that obtained with fenretinide except in the WM266-4 and U251 cells (Figure 4). There was also a reduction in GRP78 expression at the highest doses of honkokiol used in most of the cell lines (Figures 3 and 4). Expression of these ER stress and apoptosis markers in response to EGCG was marginal at best (Figure 4). These data suggest that HNK induces ER stress in neurectodermal tumour cells, possibly as a consequence of an ability to bind GRP78, and indicate that stress responses to EGCG are less well defined.

Combination treatment of melanoma and neuroblastoma cells with fenretinide and bortezomib produces synergistic effects *in vitro* and in xenograft tumour models (Hill *et al*, 2009; Pagnan *et al*, 2009). As EGCG and HNK also induce ER stress, which may, at least in part, result from an ability to interfere with the ER-stress-sensing function of GRP78, we investigated the ability of these compounds to enhance cell death in combination with fenretinide or bortezomib over 24 h treatment. There was no significant drug-dose effect on ci (linear models, $P > 0.05$ for all cell-line drug combinations). Overall, EGCG was inhibitory in combination with bortezomib regardless of cell line or cell type (Figure 5). In combination with fenretinide, EGCG was inhibitory or additive with respect to glioblastoma and neuroblastoma cells, respectively, but had mildly synergistic effects on melanoma cells. In contrast, HNK had synergistic effects on melanoma and glioblastoma cells in combination with fenretinide or bortezomib, although for neuroblastoma cells HNK had additive effects with fenretinide or inhibitory effects in combination with bortezomib (Figure 5).

In addition to cell death, the expression of GRP78 and ATF4, and the induction of caspase-3 cleavage were measured at the same time point. Although HNK or EGCG induced significant increases or decreases of these markers by comparison with fenretinide or bortezomib alone (and in some cases no change), these did not correlate in any consistent way with synergistic, additive or inhibitory effects on cell death (Figure 6). This may be a consequence of a shortened time scale for cell death at increased stress with two drugs acting in concert. Using HNK and the two melanoma lines as models, this possibility was tested by treating

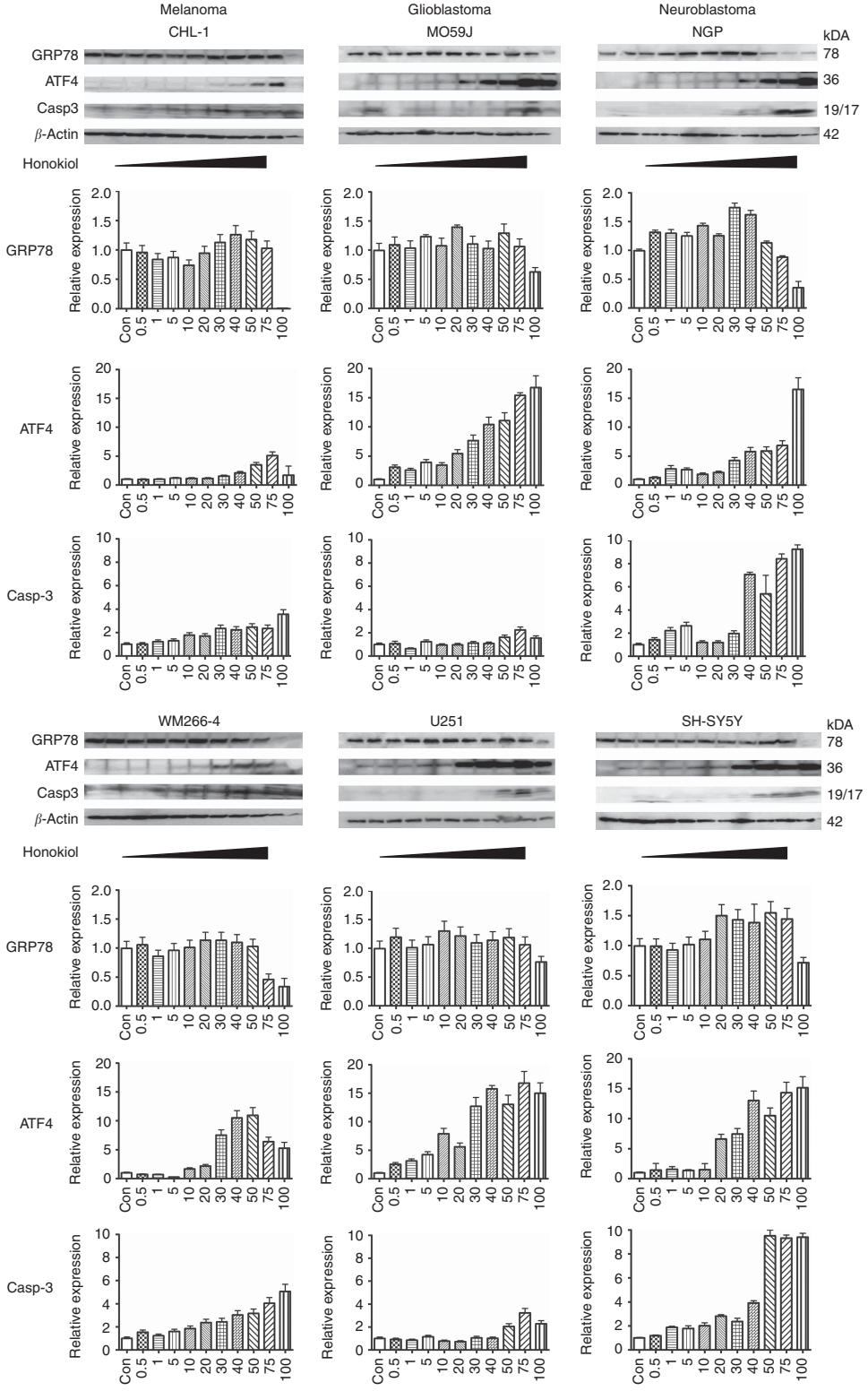

Figure 3. The effect of honokiol (HNK) dose on the induction of ER stress markers. Melanoma (left-hand column, CHL-1 and WM266-4 cell lines), glioblastoma (middle column, MO59J and U251 cell lines) and neuroblastoma (right-hand column, NGP and SH-SY5Y cell lines) cells were treated with increasing concentrations of HNK (dose range = 0–100 μM) for 24 h before western blot analysis for ER stress markers, GRP78 and ATF4, or the apoptotic marker, cleaved caspase-3. Example western blot data are shown (molecular weights of the bands are given on the right-hand side), together with graphical summaries of densitometric quantification of the relevant bands from three experiments (bar heights are means ± 95% confidence intervals) for each cell line. Densitometric data are expressed relative to β-actin as a loading control. For the graphs, common scales were used across cancer types for each protein to facilitate visual comparisons. Note that melanoma cells were the only cell type that demonstrated caspase-3 cleavage under control conditions.

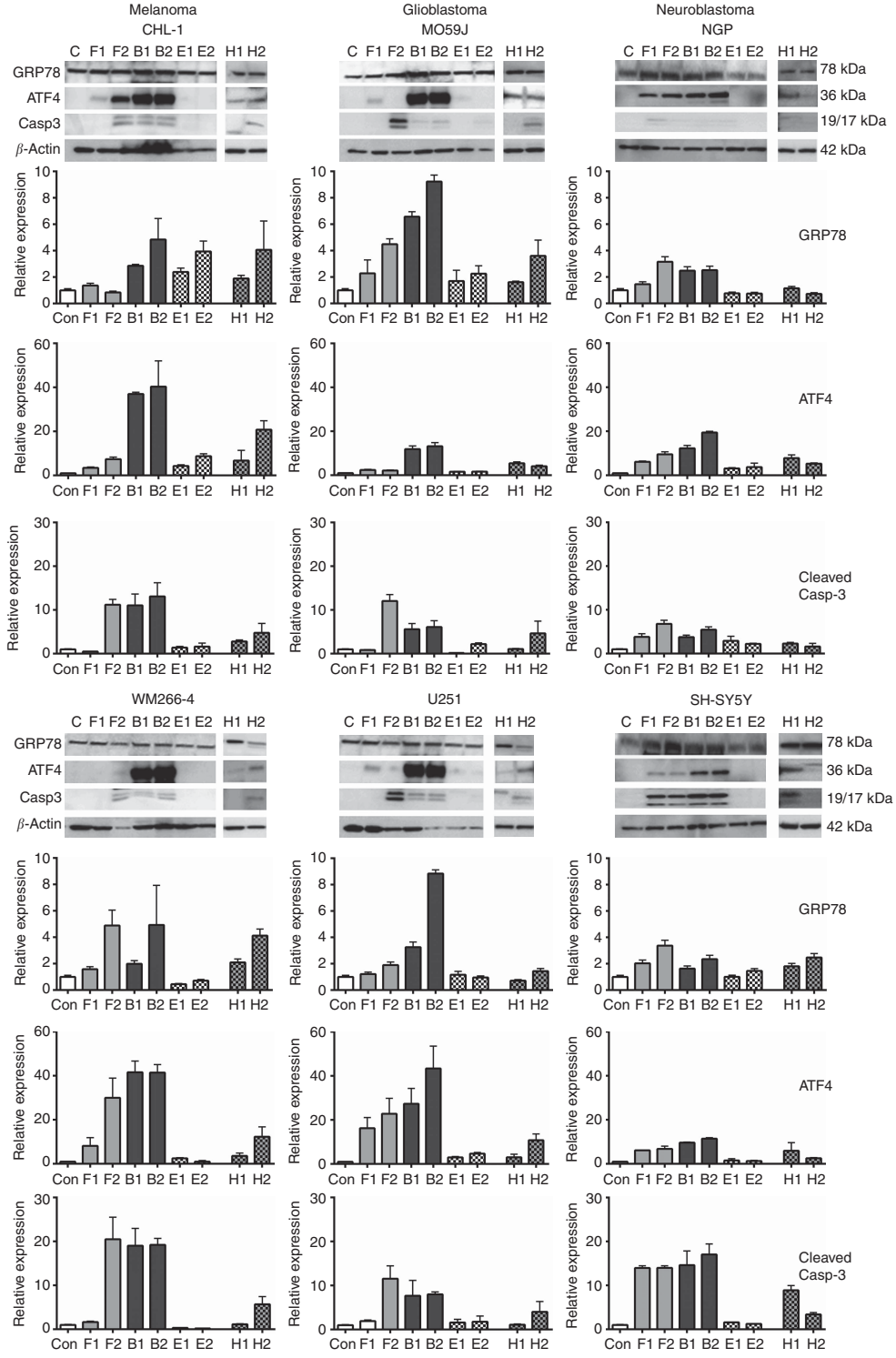

Figure 4. The effect of EGCG treatment on ER stress and apoptosis markers in comparison with fenretinide, bortezomib and honokiol using melanoma (left-hand column, cell lines as in Figure 3), glioblastoma (centre column) and neuroblastoma (right-hand column) cell lines. Cells were treated with either fenretinide (light grey bars; for melanoma and glioblastoma, F1 = 5 μM and F2 = 10 μM or neuroblastoma F1 = 2.5 μM and F2 = 5 μM), bortezomib (black bars; for melanoma and glioblastoma, B1 = 100 nM and B2 = 200 nM or neuroblastoma B1 = 10 nM and B2 = 20 nM), epigallocatechin gallate (EGCG; dotted bars, E1 = 5 μM and E2 = 10 μM) or honokiol (grey dotted bars; H1 = 50 μM and H2 = 100 μM) for 24 h. Western blot analyses were performed for GRP78 expression, induction of ATF4 and cleavage of caspase-3, using β-actin as a loading control. Example western blot data are shown (molecular weights of the bands are given on the right-hand side), together with graphical summaries of densitometric quantification of the relevant bands from three independent experiments (bar heights are means ± 95% confidence intervals) for each cell line. For the graphs, common scales were used across cancer types for each protein to facilitate visual comparisons. Honokiol experiments were done at the same time but on different blots.

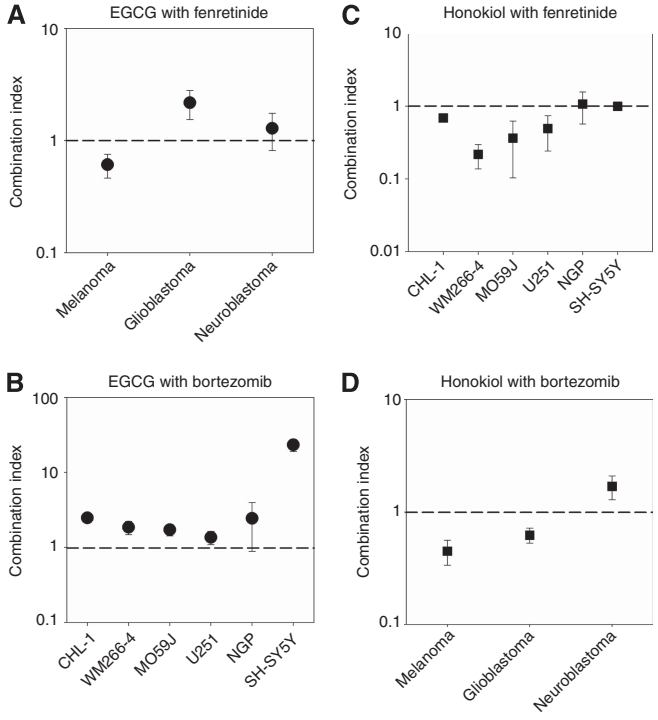

Figure 5. Synergistic, additive and inhibitory interactions on cell death in response to fenretinide or bortezomib in combination with EGCG or honokiol. Data shown are the mean and 95% confidence intervals (calculated using log-transformed values, back transformed and plotted on a log scale) for ci from each cell line and drug combination. Statistical analyses were carried out on rank-transformed data. (**A**) EGCG in combination with fenretinide—the cell type*cell line interaction was not significant ($P=0.08$), so cell types were compared using Tukey's HSD where glioblastoma and melanoma differed significantly ($P=0.022$) but there was no significant difference between neuroblastoma and glioblastoma ($P=0.3$) or melanoma ($P=0.4$). (**B**) EGCG in combination with bortezomib—celltype*cell line interaction was significant ($P=0.0002$), so data were analysed by cell line. The combination overall was inhibitory but particularly for the SH-SY5Y neuroblastoma cell line, which was significantly different to the other cell lines ($P<0.05$). (**C**) Honokiol in combination with fenretinide—cell type*cell line interaction was significant ($P=0.0031$); no difference between neuroblastoma cell lines ($P=0.9$), which were significantly different to other cell lines ($P<0.05$); WM266-4 melanoma cells were similar to glioblastoma cells ($P>0.05$) but significantly different to CHL-1 melanoma cells ($P=0.006$). (**D**) Honokiol in combination with bortezomib—no significant celltype* cell line interaction ($P=0.225$); neuroblastoma cells differed significantly from glioblastoma and melanoma cells ($P<0.0001$).

cells with HNK and fenretinide or bortezomib, and the induction of cell death after 6, 12 and 24 h, and the induction of GRP78 and ATF4 expression and caspase-3 cleavage after 6 and 12 h compared with cells treated with fenretinide, bortezomib or HNK alone (Figure 7). Cell death was time- and dose-dependent, with the level at 6 h with the combination treatments equivalent to that at 24 h for each drug alone (Figure 7). Honokiol induced markers of ER stress within 6 h. The expression of apoptosis and ER stress markers varied according to marker and drug used. For example, in CHL-1 cells, caspase-3 cleavage was increased by HNK with bortezomib at 6 h and by HNK with fenretinide at 12 h, while GRP78 and ATF4 was increased by HNK with bortezomib at 6 h and then decreased at 12 h compared with bortezomib alone (Figure 7). Clearly, the relationships between single and combination drug treatments and markers of ER stress/UPR signalling are complex and not easily interpretable in relation to the progression of cell death.

DISCUSSION

Recent studies have shown that HNK induces apoptosis of tumour cells (Arora *et al*, 2011; Cheng *et al*, 2011; Jeong *et al*, 2012; Lin *et al*, 2012). We provide evidence consistent with a mechanism of action for HNK that includes binding to the unfolded ATPase domain of GRP78 with a consequent induction of ER stress. Although EGCG and HNK both bind to the unfolded GRP78 ATPase domain, the data are consistent with HNK having the greater affinity. These results have implications for the mechanism of ER stress resulting from the interaction between either compound with GRP78 and for the potential of these natural products for development as anticancer drugs.

Binding to the ATPase domain. The observation that neither HNK nor EGCG bound to folded GRP78 deserves comment in the light of the fact that GRP78 from cell lysates was eluted from the biotinylated-HNK–streptavidin beads and the EGCG–Sepharose 4B affinity experiments reported by Ermakova *et al* (2006). In the latter case, GRP78 was incubated overnight with EGCG–Sepharose 4B before bound proteins were analysed by immunoblotting (Ermakova *et al*, 2006). It is likely that, by analogy with HSP-70 (Liu *et al*, 2010), an intrinsic mobility of the GRP78 N-terminal domain unfolds it sufficiently to facilitate access of EGCG or HNK under prolonged incubation conditions of a few hours or more. This also raises the question whether the effects of EGCG and HNK on intact cells result from binding to the ATPase domain and, if so, whether this occurs in mature ER-resident GRP78 as a result of conformational dynamics and intrinsic mobility of the ATPase domain, particularly the more-open conformational states that may interact with nucleotide exchange factors (Liu *et al*, 2010). If such intracellular interactions with the ATPase domain disrupted dynamic equilibria resulting in an increase in free PERK, IRE1 and ATF6, this would explain the induction of ER stress markers such as ATF4 by these agents, particularly HNK that induced UPR activation in melanoma cells within 6 h of treatment.

In addition, interaction between GRP78 and EGCG or HNK may occur before post-translational folding of newly synthesised GRP78. Gulow *et al* (2002) have shown that GRP78 is controlled at the translational level and propose that elevated GRP78 levels seen as part of the UPR are produced, at least in part, by increased translational efficiency of pre-existing GRP78 mRNA. These ideas imply negative effects on GRP78 synthesis resulting from the binding of HNK or EGCG to the growing polypeptide when translation of GRP78 mRNA occurs in the presence of these drugs. Possible negative effects would be stalling of translation and a reduced ability for full-length polypeptides to fold correctly into their physiologically active form. These mechanisms would be consistent with synergistic or additive effects *in vitro* when HNK is combined with antitumour agents.

Natural products as GRP78 inhibitors. As GRP78 has a key role in sensing ER stress and subsequent homeostatic responses, agents that interfere or modulate this activity may have therapeutic potential. Although EGCG (Nam *et al*, 2001) and HNK (Yu *et al*, 2012) may have other biological properties, studies showing that the AB_5 subtilase toxin, which cleaves GRP78 specifically, synergistically enhances the activity of ER stress inducers on melanoma cells (Martin *et al*, 2010) support the idea that chemical inhibitors of GRP78 may be effective as chemotherapeutic drugs. Nevertheless, although EGCG induces cell death and can overcome resistance to chemotherapeutic drugs (Ermakova *et al*, 2006; Virrey *et al*, 2008), on the basis of the present studies it did not have useful properties in combination with agents that induce ER stress. As

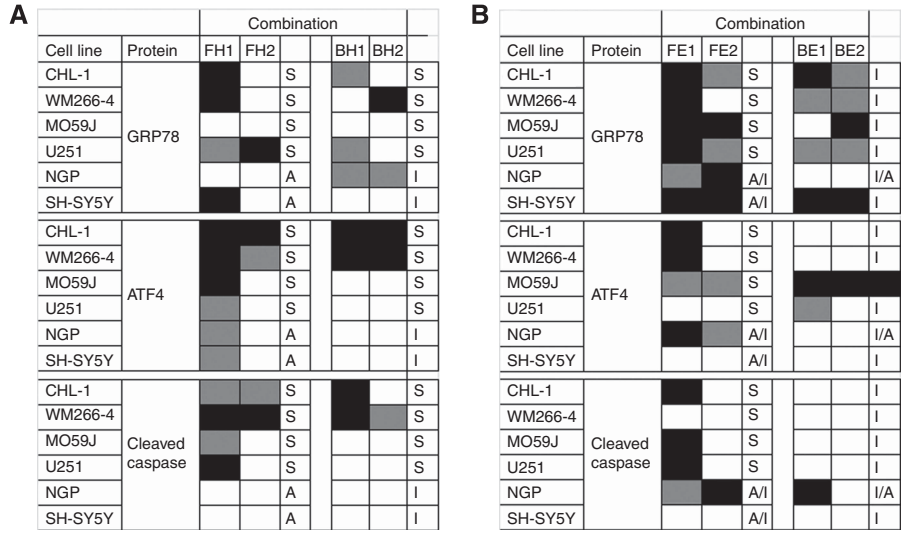

Figure 6. Summary of the effect of GRP78 inhibition by honokiol (A) or EGCG (B) treatment, on the induction of ER stress in neural-crest-derived cancer cells in response to fenretinide (F) or bortezomib (B). Data are comparisons between controls and treated cells for three experiments where a black cell indicates a significant increase ($P<0.05$), white indicates a significant decrease ($P<0.05$) or grey no significant difference ($P>0.05$) in protein expression. Status with respect to the effect of drug interactions on cell death (see Figure 5) is indicated to the right of each greyscale block: A = additivity; I = inhibition; S = synergy.

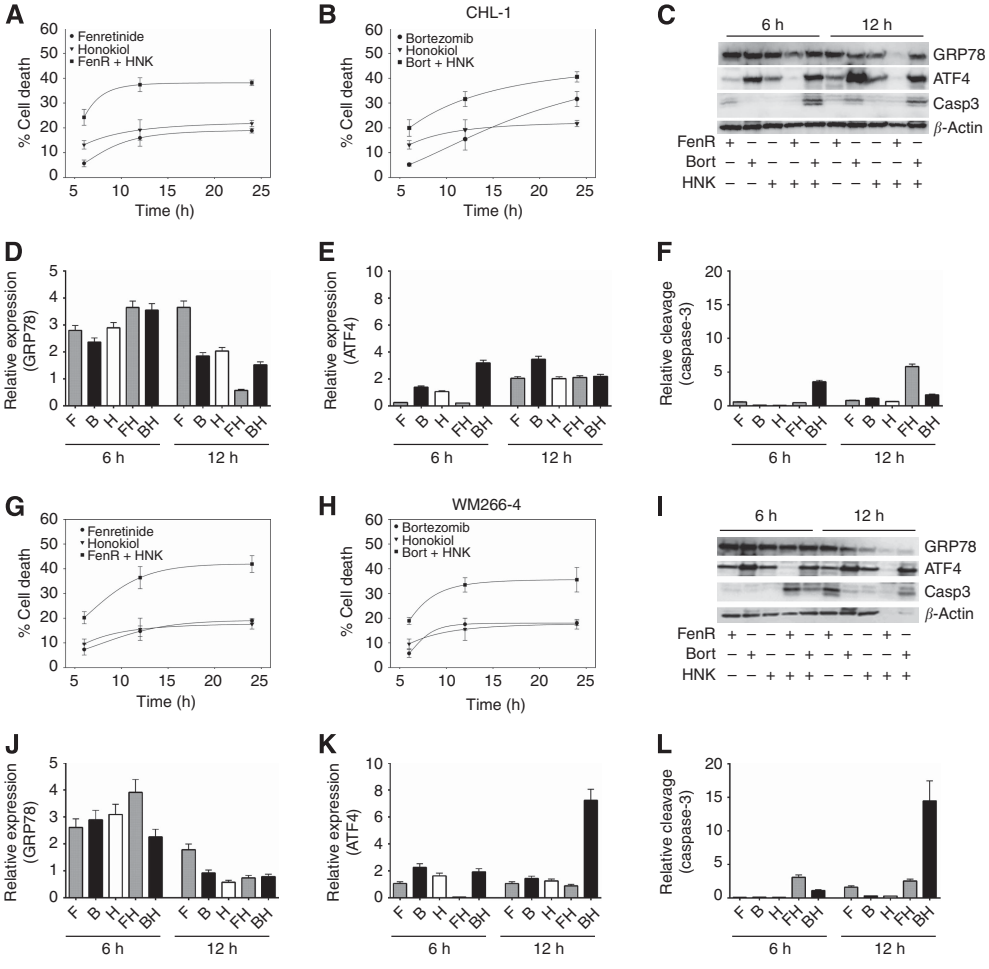

Figure 7. Time course for the effect of honokiol (HNK) on ER stress-induced cell death and the expression of markers of ER stress and apoptosis in CHL-1 (A–F) and WM266-4 (G–L) melanoma cells. Cells were treated with fenretinide (10 μM), bortezomib (Bort, 200 nM) or HNK (50 μM) for 6, 12 or 24 h, alone or in combination before analysis. Cell death was analysed by flow cytometry for fenretinide or HNK alone or in combination (**A**, **G**), bortezomib or HNK alone or in combination (**B**, **H**), and the expression of GRP78, ATF4 and caspase-3 cleavage analysed by western blotting (**C**, **I**). Graphical summaries of densitometric quantification relative to the β-actin loading control from three experiments (bar heights are means ± 95% confidence intervals) for each cell line are shown for GRP78 (**D**, **J**), ATF4 (**E**, **K**) and caspase-3 cleavage (**F**, **L**).

EGCG, like bortezomib, may also inhibit proteasome activity (Nam *et al*, 2001), the inhibitory effect of EGCG on bortezomib activity could result from competitive interactions at the proteasome active site; how such interference might reduce the subsequent transition to cell death is unknown. In many respects, EGCG was also less effective than HNK, with greater variability between cell lines in sensitivity to EGCG-induced cell death and lower induction of ER stress markers. In contrast to EGCG, HNK had synergistic effects with fenretinide or bortezomib on melanoma and glioblastoma cells. The greater effectiveness of HNK at inducing ER stress was consistent with DSC data indicating greater efficacy of HNK for binding to the unfolded ATPase domain. Recent studies have also shown that HNK can cross the blood–brain barrier (Lin *et al*, 2012), and thus may be a useful adjunct to conventional chemotherapy in the treatment of brain tumours.

Clearly, HNK may warrant further development, either as a single drug or as a means to increase efficacy in combination with other antitumour drugs, but this will depend on tumour type. The combination effects of HNK or EGCG could not be related to changes in stress signalling, and the data suggest complex interrelationships between the effects of different drugs and drug combinations and the time-dependent progression of drug-induced cell death. Given the evidence for a direct interaction between HNK or EGCG and the ATPase domain of GRP78, studies are required to identify the interacting domains and how these compounds modify conformational dynamics of GRP78 in the context of the mature ER-resident and newly synthesised forms. These will be important in the use of these compounds, particularly HNK, as it leads for further development of drugs targeting GRP78 to induce ER stress in cancer cells.

ACKNOWLEDGEMENTS

We thank and acknowledge Cancer Research UK (grant number C1376/A9254) for funding the cell-line studies, and NIH grant RO1 AR47901 for funding the affinity and protein identification work reported in this paper.

REFERENCES

Arbiser JL, Moses MA, Fernandez CA, Ghiso N, Cao Y, Klauber N, Frank D, Brownlee M, Flynn E, Parangi S, Byers HR, Folkman J (1997) Oncogenic H-ras stimulates tumor angiogenesis by two distinct pathways. *Proc Natl Acad Sci USA* **94**: 861–866.

Armstrong JL, Flockhart R, Veal GJ, Lovat PE, Redfern CP (2010) Regulation of endoplasmic reticulum stress-induced cell death by ATF4 in neuroectodermal tumor cells. *J Biol Chem* **285**: 6091–6100.

Arora S, Bhardwaj A, Srivastava SK, Singh S, McClellan S, Wang B, Singh AP (2011) Honokiol arrests cell cycle, induces apoptosis, and potentiates the cytotoxic effect of gemcitabine in human pancreatic cancer cells. *PLoS One* **6**: e21573.

Bertolotti A, Zhang Y, Hendershot LM, Harding HP, Ron D (2000) Dynamic interaction of BiP and ER stress transducers in the unfolded-protein response. *Nat Cell Biol* **2**: 326–332.

Blais JD, Filipenko V, Bi M, Harding HP, Ron D, Koumenis C, Wouters BG, Bell JC (2004) Activating transcription factor 4 is translationally regulated by hypoxic stress. *Mol Cell Biol* **24**: 7469–7482.

Chen YJ, Wu CL, Liu JF, Fong YC, Hsu SF, Li TM, Su YC, Liu SH, Tang CH (2010) Honokiol induces cell apoptosis in human chondrosarcoma cells through mitochondrial dysfunction and endoplasmic reticulum stress. *Cancer Lett* **291**: 20–30.

Cheng N, Xia T, Han Y, He QJ, Zhao R, Ma JR (2011) Synergistic antitumor effects of liposomal honokiol combined with cisplatin in colon cancer models. *Oncol Lett* **2**: 957–962.

Cooper A (2001) Differential scanning microcalorimetry. In *Protein-Ligand Interactions: Hydrodynamics and Calorimetry*, Harding SE, Chowdry BZ (eds) pp 287–317. Oxford University Press: Oxford.

Corazzari M, Lovat PE, Oliverio S, Pearson AD, Piacentini M, Redfern CP (2003) Growth and DNA damage-inducible transcription factor 153 mediates apoptosis in response to fenretinide but not synergy between fenretinide and chemotherapeutic drugs in neuroblastoma. *Mol Pharmacol* **64**: 1370–1378.

Ermakova SP, Kang BS, Choi BY, Choi HS, Schuster TF, Ma WY, Bode AM, Dong Z (2006) (-)-Epigallocatechin gallate overcomes resistance to etoposide-induced cell death by targeting the molecular chaperone glucose-regulated protein 78. *Cancer Res* **66**: 9260–9269.

Gulow K, Bienert D, Haas IG (2002) BiP is feed-back regulated by control of protein translation efficiency. *J Cell Sci* **115**: 2443–2452.

Haselsberger K, Peterson DC, Thomas DG, Darling JL (1996) Assay of anticancer drugs in tissue culture: comparison of a tetrazolium-based assay and a protein binding dye assay in short-term cultures derived from human malignant glioma. *Anti-Cancer Drugs* **7**: 331–338.

Hill DS, Martin S, Amnstrong JL, Flockhart R, Tonison JJ, Simpson DG, Birch-Machin MA, Redfern CPF, Lovat PE (2009) Combining the endoplasmic reticulum stress-inducing agents bortezomib and fenretinide as a novel therapeutic strategy for metastatic melanoma. *Clin Cancer Res* **15**: 1192–1198.

Jeong JJ, Lee JH, Chang KC, Kim HJ (2012) Honokiol exerts an anticancer effect in T98G human glioblastoma cells through the induction of apoptosis and the regulation of adhesion molecules. *Int J Oncol* **41**: 1358–1364.

Lamb HK, Leslie K, Dodds AL, Nutley M, Cooper A, Johnson C, Thompson P, Stammers DK, Hawkins AR (2003) The negative transcriptional regulator NmrA discriminates between oxidized and reduced dinucleotides. *J Biol Chem* **278**: 32107–32114.

Lamb HK, Mee C, Xu W, Liu L, Blond S, Cooper A, Charles IG, Hawkins AR (2006) The affinity of a major Ca2+ binding site on GRP78 is differentially enhanced by ADP and ATP. *J Biol Chem* **281**: 8796–8805.

Lee AS (2007) GRP78 induction in cancer: therapeutic and prognostic implications. *Cancer Res* **67**: 3496–3499.

Lin JW, Chen JT, Hong CY, Lin YL, Wang KT, Yao CJ, Lai GM, Chen RM (2012) Honokiol traverses the blood-brain barrier and induces apoptosis of neuroblastoma cells via an intrinsic bax-mitochondrion-cytochrome c-caspase protease pathway. *Neuro Oncol* **14**: 302–314.

Liu Y, Gierasch LM, Bahar I (2010) Role of Hsp70 ATPase domain intrinsic dynamics and sequence evolution in enabling its functional interactions with NEFs. *PLoS Comput Biol* **6**: e1000931.

Martin S, Hill DS, Paton JC, Paton AW, Birch-Machin MA, Lovat PE, Redfern CP (2010) Targeting GRP78 to enhance melanoma cell death. *Pigment Cell Mel Res* **23**: 675–682.

Nam S, Smith DM, Dou QP (2001) Ester bond-containing tea polyphenols potently inhibit proteasome activity in vitro and in vivo. *J Biol Chem* **276**: 13322–13330.

Pagnan G, Di Paolo D, Carosio R, Pastorino F, Marimpietri D, Brignole C, Pezzolo A, Loi M, Galietta LJ, Piccardi F, Cilli M, Nico B, Ribatti D, Pistoia V, Ponzoni M (2009) The combined therapeutic effects of bortezomib and fenretinide on neuroblastoma cells involve endoplasmic reticulum stress response. *Clin Cancer Res* **15**: 1199–1209.

Paton AW, Beddoe T, Thorpe CM, Whisstock JC, Wilce MCJ, Rossjohn J, Talbot UM, Paton JC (2006) AB(5) subtilase cytotoxin inactivates the endoplasmic reticulum chaperone BiP. *Nature* **443**: 548–552.

Paton AW, Paton JC (2010) *Escherichia coli* subtilase cytotoxin. *Toxins* **2**: 215–228.

R Development Core Team (2012) *R: A Language and Environment for Statistical Computing*. R Foundation for Statistical Computing: Vienna, Austria.

Rao RV, Peel A, Logvinova A, del Rio G, Hermel E, Yokota T, Goldsmith PC, Ellerby LM, Ellerby HM, Bredesen DE (2002) Coupling endoplasmic reticulum stress to the cell death program: role of the ER chaperone GRP78. *FEBS Lett* **514**: 122–128.

Reddy RK, Mao C, Baumeister P, Austin RC, Kaufman RJ, Lee AS (2003) Endoplasmic reticulum chaperone protein GRP78 protects cells from apoptosis induced by topoisomerase inhibitors: role of ATP binding site in suppression of caspase-7 activation. *J Biol Chem* **278**: 20915–20924.

Remotti F, Fetsch JF, Miettinen M (2001) Keratin 1 expression in endothelia and mesenchymal tumors: an immunohistochemical analysis of normal and neoplastic tissues. *Hum Pathol* **32**: 873–879.

Ritz C, Streibig JC (2005) Bioassay analysis using R. *J Stat Software* **12**(5).

Samali A, Fitzgerald U, Deegan S, Gupta S (2010) Methods for monitoring endoplasmic reticulum stress and the unfolded protein response. *Int J Cell Biol* **2010**: 830–837.

Schroder M (2005) The mammalian unfolded protein response. *Annu Rev Biochem* **74**: 739–789.

Schroder M (2006) The unfolded protein response. *Mol Biotechnol* **34**: 279–290.

Schroder M, Kaufman RJ (2005) ER stress and the unfolded protein response. *Mutat Res* **569**: 29–63.

Shen J, Chen X, Hendershot L, Prywes R (2002) ER stress regulation of ATF6 localization by dissociation of BiP/GRP78 binding and unmasking of Golgi localization signals. *Dev Cell* **3**: 99–111.

Stammers DK, Ren J, Leslie K, Nichols CE, Lamb HK, Cocklin S, Dodds A, Hawkins AR (2001) The structure of the negative transcriptional regulator NmrA reveals a structural superfamily which includes the short-chain dehydrogenase/reductases. *EMBO J* **20**: 6619–6626.

Virrey JJ, Dong D, Stiles C, Patterson JB, Pen L, Ni M, Schönthal AH, Chen TC, Hofman FM, Lee AS (2008) Stress chaperone GRP78/BiP confers chemoresistance to tumor-associated endothelial cells. *Mol Cancer Res* **6**: 1268–1275.

Yu C, Zhang Q, Zhang HY, Zhang X, Huo X, Cheng E, Wang DH, Arbiser JL, Spechler SJ, Souza RF (2012) Targeting the intrinsic inflammatory pathway: honokiol exerts proapoptotic effects through STAT3 inhibition in transformed Barrett's cells. *Am J Physiol Gastrointest Liver Physiol* **303**: G561–G569.

Zhao X, Hume SL, Johnson C, Thompson P, Huang J, Gray J, Lamb HK, Hawkins AR (2010) The transcription repressor NmrA is subject to proteolysis by three *Aspergillus nidulans* proteases. *Protein Sci* **19**: 1405–1419.

Supplementary Information accompanies this paper on British Journal of Cancer website (http://www.nature.com/bjc)